Rolando Cárdenas · Vladimir Mochalov
Oscar Parra · Osmel Martin *Editors*

Proceedings of the 2nd International Conference on BioGeoSciences

Modeling Natural Environments

Springer

Proceedings of the 2nd International Conference on BioGeoSciences

Rolando Cárdenas · Vladimir Mochalov
Oscar Parra · Osmel Martin
Editors

Proceedings of the 2nd International Conference on BioGeoSciences

Modeling Natural Environments

Springer

Editors
Rolando Cárdenas
Universidad Central "Marta Abreu"
de Las Villas
Santa Clara, Cuba

Vladimir Mochalov
Institute for Cosmophysical Research
Kamchatka, Russia

Oscar Parra
University of Concepción
Concepción, Chile

Osmel Martin
Universidad Central "Marta Abreu"
de Las Villas
Santa Clara, Cuba

ISBN 978-3-030-04232-5 ISBN 978-3-030-04233-2 (eBook)
https://doi.org/10.1007/978-3-030-04233-2

Library of Congress Control Number: 2018961690

This Springer imprint is published by the registered company Springer Nature Switzerland AG
The registered company address is: Gewerbestrasse 11, 6330 Cham, Switzerland

Contents

On the Quantification of Habitability: Current Approaches

Rolando Cárdenas, Rosmery Nodarse-Zulueta, Noel Perez, Daile Avila-Alonso and Osmel Martin

Abstract In this chapter, we outline general ideas to quantify habitability, starting with a general abiogenesis–biogenesis conceptual model. We connect this model with the approach of the astrobiological school of quantitative habitability, specifically with quantitative habitability theory, to devise habitability indexes. We present two indexes devised by us: the Aquatic Primary Habitability for photosynthesis-based ecosystems, and the Chemosynthetic Habitability Index for chemoautotrophy-based ones. As a case study, we present the application of the last one to hydrothermal vents. It is also mentioned the possibility of embedding parameters such as net primary productivity, calculated using habitability indexes, into greater ecological models with several trophic models, making a clear connection between the astrobiological and ecological approaches of quantitative habitability.

Keywords Abiogenesis–biogenesis model · Quantitative habitability theory Habitability index

1 Introduction

Quantitative habitability remains an open issue. Currently, there are three (complementary) approaches to quantify habitability. In the astrobiological, the main premises for life origin (abiogenesis) and evolution (biogenesis) are studied. In the biogeochemical, emphasis is put on biogeochemical cycles and the availability of nutrients and energy, while in the ecological a closer look is put at the interactions between the species in the context of the ecosystem [1]. However, due to the complexity of life, the quantification of habitability is still a very open science. Thus, our aim in this paper is to launch some ideas on how to quantify habitability

R. Cárdenas (✉) · R. Nodarse-Zulueta · N. Perez · D. Avila-Alonso · O. Martin
Planetary Science Laboratory, Universidad Central "Marta Abreu" de Las Villas, Santa Clara, Cuba
e-mail: rcardenas@uclv.edu.cu

R. Cardenas et al. (eds.), *Proceedings of the 2nd International Conference on BioGeoSciences*, https://doi.org/10.1007/978-3-030-04233-2_1

in the spirit of this II International Conference on BioGeoSciences (BG-17): from the small molecular–cellular scales to the enormous astrobiological–cosmological ones.

We work with the hypothesis that the current level of knowledge of mankind allows generalizations concerning life in the Universe. So, accepting the principle of world's material unity (the most basic laws of Nature, formulated by physics and chemistry, are valid in the whole observed Universe, which is supported by a wide set of astrophysical observations), I propose a conceptual model for abiogenesis (life origin)–biogenesis (life evolution), in principle valid for the entire observed Universe. From [2, 3] the main ingredients of this model can be inferred, i.e., life needs:

(1) Biogenic chemical elements (for instance, CHON in Earth): the chemical (mineral) aspect of life;
(2) A liquid medium (solvent) for the biogenic elements properly mix to form biomolecules (water on Earth): the mixing (kinetic) aspect of life;
(3) An energy source for the above-mentioned mix proceeds at a proper speed, to keep low entropy and to perform work (light for photosynthesis, redox chemical energy for chemosynthesis): the energetic (thermodynamic) aspect of life;
(4) An appropriate physicochemical environment allowing formed biological molecules to persist, for instance; adequate temperature range, radiational regime, etc., the physicochemical aspect of life.

Rocky planetary bodies (either planets or satellites) are the places in the Universe in which above-mentioned premises are more likely to be fulfilled. It is very difficult to infer when they first formed, some authors saying that around 1–2 Gy after the Big Bang were necessary, while others state that 10–17 million could have been enough [4].

2 The Quantification of Habitability

The main postulate of the (astrobiological) quantitative habitability theory [5] states that habitability indexes HI can be constructed as a product of environmental functions $f_i(\{x_j\})$ which depend on sets of environmental variables $\{x_j\}$:

$$\mathrm{HI} = \prod_{i=1}^{n} f_i\left(\{x_j\}\right) \tag{1}$$

Typically, an HI is normalized so that it ranges between 0 (dead environment) and 1 (optimum for life). A crucial fact is that a properly devised HI can be used to assess the net primary productivity NPP (rate at which non-living matter transforms into living matter) of an environment:

$$\mathrm{NPP} = \mathrm{HI} \cdot \mathrm{NPP}_{\max} \tag{2}$$

where $\mathrm{NPP}_{\max}$ is the maximum NPP.

Relating the main postulate of quantitative habitability theory with the conceptual model for abiogenesis–biogenesis, a generic habitability index can be written as:

$$\mathrm{HI} = f_M f_K f_E f_{\mathrm{PC}} \tag{3}$$

where f_M, f_K, f_E, and f_{PC} are functions representing the mineral, kinetic, energetic, and physicochemical aspects of life, respectively. For each of these aspects, we have used several functions, some devised by other authors, some devised by us. However, in order to build an HI, as in every model of Nature, we just include the functions of those variables which limit habitability; otherwise, the model could be untreatable from the mathematical point of view. For instance, an HI for a terrestrial ecosystem can include a function of the solvent water $f(\mathrm{H_2O})$, but in an aquatic ecosystem water is not limiting but optimum, which allows to disregard this function or, more properly, to set $f(\mathrm{H_2O}) = 1$. Another issue is to consider the interactions (feedbacks) between variables.

2.1 The Aquatic Primary Habitability Index

Using the methodology of the former section, we investigated the (primary) habitability of aquatic ecosystems. It is usually acknowledged that the main environmental variables controlling life in these ecosystems are light, nutrients, temperature, and salinity. Then, we propose an HI for aquatic environments without salt stress, the Aquatic Primary Habitability (APH):

$$\mathrm{APH} = f(L) f(N) f(T) \tag{4}$$

where $f(L)$, $f(N)$, and $f(T)$ are functions of light, limiting nutrient, and temperature, respectively. Particular versions of this index are:

$$\mathrm{APH_I} = f(L) f(T) \tag{5}$$

and

$$\mathrm{APH_{II}} = f(L) f(N) \tag{6}$$

The index represented in Eq. (5) was applied to environments where light, rather than nutrients, is a limiting variable [6]. Common examples are rocky planets and satellites orbiting red dwarfs, stars with a light emission much smaller than emission of solar-type stars.

The index represented by Eq. (6) was applied to Ana Maria Gulf, a Cuban gulf of importance for tourism and fisheries [7]. The function of light was inspired in the *E* model for photosynthesis [8]:

$$\frac{P(z)}{P_S} = \frac{1 - \exp(-E_{PAR}(z)/E_S)}{1 + E^*_{UV}(z)} \tag{7}$$

where $P(z)$ and P_S are the photosynthesis rates at depth z and the maximum possible, respectively. $E_{PAR}(z)$ and $E^*_{UV}(z)$ are the irradiances of photosynthetically active radiation (PAR) and ultraviolet radiation (UV) at depth z, respectively. Spectral UV irradiances are convolved with a biological action spectrum weighting the inhibitory effect on photosynthesis of each wavelength, which is indicated by the asterisk. E_S is a parameter of photosynthetic efficiency: the smaller its value, the greater the efficiency of the species to use PAR. Photosynthesis rates are depth-dependent, so the actual $f(L)$ we use in the aquatic habitability indexes presented above is an average in all the photic zone normalized respect to the optimum average:

$$f(L) = \left\langle \frac{P(z)}{P_S} \right\rangle \Big/ \left\langle \frac{P(z)}{P_S} \right\rangle_{opt} \tag{8}$$

The calculation of the optimum average was presented in Cardenas et al. [6]. The function on nutrients used in Eq. (6) was inspired in an eutrophication index [7, 9].

2.2 A Chemosynthetic Habitability Index

To devise a chemosynthetic habitability index (QHI), we propose to substitute the light function $f(L)$ in APH by a function of the chemical energy $f(Q)$, which chemoautotrophic organisms are able to use:

$$\text{QHI} = f(Q)f(N)f(T) \tag{9}$$

The form of the chemical function $f(Q)$ can be inspired by suggested analogies between photosynthesis and chemosynthesis, as can be seen in Figs. 3 and 4 by Shock and Holland [1]. Ignoring the (still undetected) last stage of chemoinhibition in above-mentioned Fig. 4, we suggest, by analogy with the non-inhibitory part of the *E* model for photosynthesis, the following chemical function [10, 11]:

$$f(Q) = 1 - e^{-\frac{I}{q}} \tag{10}$$

where I is the chemical energy per unit area and per unit time that the chemoautotrophic organism receives, and q is a parameter of chemosynthetic efficiency.

The function of nutrients $f(N)$ is inspired in the well-known Michaelis–Menten kinetics (normalizing respect to its maximum value):

$$f(N) = \frac{v_{\max}[\mathrm{LN}]/(K_{\mathrm{M}} + [\mathrm{LN}])}{f_{\max}(N)} \tag{11}$$

where [LN] stands for the concentration of limiting nutrient, $v_{\max}$ is the maximum assimilation rate of the limiting nutrient, and K_{M} is the semi-saturation constant known as Michaelis constant.

As a function of temperature $f(T)$, we take an inverted parabola symmetric respect to the optimum temperature for life T_{opt} [12]:

$$f(T) = 1 - \left(\frac{T_{\mathrm{opt}} - T}{T_{\mathrm{opt}} - 273}\right)^2 \tag{12}$$

3 Case Studies

We have applied habitability indexes to several scenarios, which can be divided into extraterrestrial, of Earth's geological history, current Earth and Cuban context. In Chap. 8 of these proceedings, the reader can find a detailed application of our Aquatic Primary Habitability to the Gulf of Ana Maria in Cuba, a photosynthesis-based ecosystem. Thus, in this chapter we present the application to a chemosynthesis-based ecosystem: the black smoker TY, located at 2.3 km depth in the East Pacific Ridge. Hydrothermal vents can host very dynamic ecosystems, mostly supported by chemosynthesis, although low levels of photosynthesis from geothermal photons have been reported by Perez et al. [13] and Das et al. [14]. Typically, the reaction which most contributes to chemosynthesis is the oxidation of hydrogen sulfide:

$$\mathrm{H_2S} + 2\mathrm{O_2} \rightarrow \mathrm{SO_4^{2-}} + 2\mathrm{H^+} \tag{13}$$

in which the limiting reactant is dioxygen. This is an extremely rich source of energy for chemoautotrophs, releasing a free energy:

$$\Delta G = 794\ \mathrm{kJ/mol} \tag{14}$$

To calculate I, we considered that the geometry of the hydrothermal fluid or effluent is a plane and that the reactants diffuse from it to both right and left directions in imaginary planes parallel to the hydrothermal fluid plane. Then, the Fick law was used to calculate the fluxes φ of dioxygen:

$$\varphi = -D\frac{\mathrm{d}[O_2]}{\mathrm{d}x} \tag{15}$$

where D is the diffusion coefficient of dioxygen, $[O_2]$ is its concentration, and x is the distance from the hydrothermal fluid plane. The intensity I is found from:

$$I = \varphi \Delta G \tag{16}$$

For the calculation of $f(Q)$, it was assumed a null concentration of dioxygen in the vent and a constant increase up to 5.0 mg/mol at 2.5 m from it. It was also considered the dependence on temperature of the diffusion coefficient D. For the calculation of the temperature function $f(T)$, it was assumed that the optimum temperature for living organisms is 298 K (25 °C), while for the calculation of the nutrients function $f(N)$ we considered the wide range of variation of nitrogen concentration $[N]$ in hydrothermal vents: 10, 100, and 1000 μmol/L. Then, the chemosynthetic habitability index (QHI) was calculated, and Figs. 1, 2, and 3 show the results.

From all three plots, we see that chemosynthetic habitability is highly sensitive to temperature and to the parameter of chemosynthetic efficiency q, while it shows little sensitivity to the concentration of nitrogen (limiting nutrient). However, it should be noticed that the value taken for the Michaelis constant K_M for the evaluation of the function of nutrients is one reported for a generic phytoplankton organism [15], given the scarcity of corresponding data for chemoautotrophs.

We have presented a first habitability index for chemosynthesis-based ecosystems, specifically for chemoautotrophy-based ones. The index has the spirit of quantitative habitability from an astrobiological perspective. Its mathematical form can be considered quite general, although some refinements can be done. Its application to a case study, hydrothermal vents, showed high sensitivity of chemoautotrophic life to temperature and to the parameter q, which characterizes the efficiency with which chemical energy is used by the chemoautotrophs. Scarcity

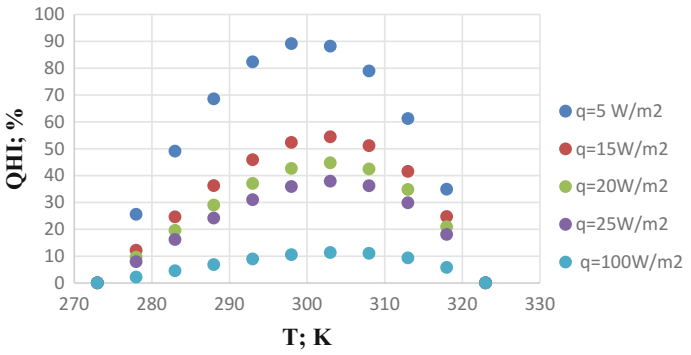

Fig. 1 Chemosynthetic habitability versus temperature for $[N]$ = 10 μmol/L

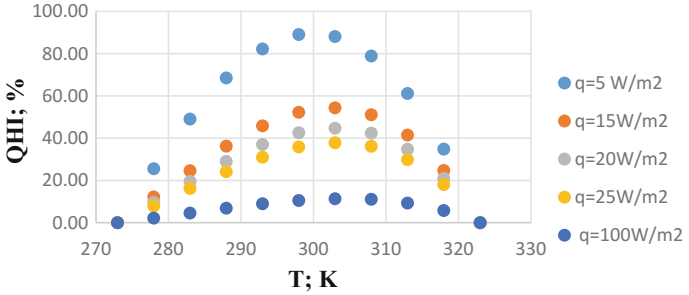

Fig. 2 Chemosynthetic habitability versus temperature for [*N*] = 100 μmol/L

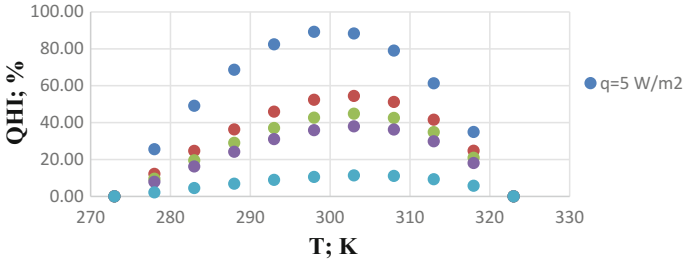

Fig. 3 Chemosynthetic habitability versus temperature for [*N*] = 1000 μmol/L

of data for these organisms still limits the refinement and applications of the index, especially in the deep biosphere. We hope that ongoing and planned expeditions involving deep sea and continental crust drilling will improve this situation.

On another hand, using Eq. (2) it is possible to estimate parameters, such as net primary productivity, for both photosynthesis- or chemosynthesis-based ecosystems. It is also possible to embed these parameters into greater ecological models, making a clear connection between the astrobiological and ecological approaches of quantitative habitability. In Chap. 8 of this book, an explicit example is presented.

4 Conclusions

In this chapter, we outlined a methodology to quantify habitability. It incorporates ideas from the astrobiological school, specifically quantitative habitability theory; to devise habitability indexes valid either for photosynthesis-based ecosystems or for chemoautotrophy-based ones. Applications to cases studies are presented or mentioned. It is also suggested to embed the parameters calculated using habitability indexes into ecological models of trophic levels. This also shows the applicability of quantitative habitability theory to spatial–temporal scales typical in ecological

studies, showing a useful bridge between astrobiology and ecology. In forthcoming publications, refinements of this methodology will be presented, as well as its applications to case studies.

References

1. Shock E, Holland M (2007) Quantitative habitability. Astrobiology 7:839
2. Schulze-Makuch D, Irwin L (2008) Life in the Universe. Springer-Verlag, Berlin Heidelberg, Germany
3. Raven J, Cockell C, Kaltenegger L (2011) Energy sources for, and detectability of, life on extrasolar planets. Capítulo del libro genesis-in the beginning: precursors of life, chemical models and early biological evolution. Springer, Amsterdam
4. Loeb A (2014) The habitable epoch of the early universe. Int J Astrobiol 13:337
5. Méndez A (2010) Evolution of the global terrestrial habitability during the last century. Proceedings of sixth astrobiology science conference, Houston, TX, USA, pp 26–29
6. Cardenas R, Pérez-Díaz N, Martínez-Frias J, Martín-González O (2014) On the habitability of aquaplanets. Challenges 5:284
7. Álvarez-Salgueiro J (2015) Productividad primaria del fitoplancton en el golfo de Ana María, Cuba. B.Sc. Thesis in Physics. Supervisors: Dailé Avila-Alonso-Alonso & Rolando Cardenas. Consultant: Roberto González-de Zayas. Available at http://dspace.uclv.edu.cu:8089/
8. Fritz J, Neale P, Davis R, Pelloquin J (2008) Response of Antarctic phytoplankton to solar UVR exposure: inhibition and recovery of photosynthesis in coastal and pelagic assemblages. Mar Ecol Prog Ser 365:1
9. Karydis M, Ignatiades L, Moschopoulou N (1983) An index associated with nutrient eutrophication in the marine environment. Estuar Coast Shelf Sci 16:339
10. Cardenas R, Pérez Díaz N, Avila-Alonso D, Nodarse-Zulueta R (2017) ¿Se originó la vida en el eón Hadeico? ¿De manera fotosintética o quimiosintética? Memorias de la VII Convención de Ciencias de la Tierra, Abril/2017, La Habana, Cuba. Available at http://www.cubacienciasdelatierra.com/es/general15
11. Nodarse-Zulueta R (2017) Diseño de un Indice de Habitabilidad Quimiosintética. B.Sc. Thesis. Supervisors: Rolando Cardenas and Noel Pérez Díaz. Consultant: Dailé Avila-Alonso. Available at http://dspace.uclv.edu.cu:8089/
12. Volk T (1987) Feedbacks between weathering and atmospheric CO_2 over the last 100 million years. Am J Sci 287:763
13. Pérez N, Cardenas R, Martin O, Leiva-Mora M (2013) The potential for photosynthesis in hydrothermal vents: a new avenue for life in the Universe? Astrophys Space Sci 346:327–331
14. Das A, Singh T, LokaBharathi P, Dhakephalkar P, Mallik S, Kshirsagar P, Khadge N, Nagender Nath B, Bhattacharya S, Kumar Dagar A, Kaur P, Ray D, Shukla A, Fernandes C, Fernandes S, Thomas T, Mamatha S, Shashikant Mourya B, Murti Meena R (2017) Astrobiological implications of dim light phototrophy in deep-sea red clays. Life Sci Space Res 12:39–50
15. Amemiya T, Enomoto T, Rossberg A, Yamamoto T, Inamori Y, Itoh K (2007) Stability and dynamical behaviour in a real lake model and implications for regime shifts in real lakes. Ecol Model 206:54

The Dynamical Systems Approach to Modeling: The Universe as a Case Study

Ailier Rivero-Acosta, Adrian Linares-Rodriguez and Carlos R. Fadragas

Abstract The acceleration of the expansion of the Universe, as it is indicated by observations of redshift of light coming from supernovas, anisotropies of cosmological microwave background radiation, and the large-scale structure of the Universe, defines one of the most interesting theoretical problems that is facing the modern cosmology. The aim of this work is to show the analysis of the idea that inflation and dark energy are two subjects closely related, that is, both equivalents to the fundamental scalar field known as the standard model Higgs field. We considered that there exist non-trivial solutions with non-minimal coupling of the Cosmological Higgs Field to gravity. For this condition, an attractive cosmological model was derived. Results from applying the dynamical stability analysis show that the current accelerated expansion of the Universe is one of several possibilities. The future behavior of the Universe could seriously affect the existence of particles and structures that we are made of. For that reason, it is important to do some comments on this idea.

Keywords Cosmological Higgs Field · Dynamical systems · Accelerated expansion

1 Introduction

The acceleration of the expansion of the late Universe, as it is indicated by observations [1–6], defines one of the deepest theoretical problems that is facing modern cosmology. In July 2012 was announced the observation of the Higgs boson at the CERN. Then, it is a very stimulating task to build a cosmological model that includes the Cosmological Higgs Field non-minimally coupled to

A. Rivero-Acosta (✉) · A. Linares-Rodriguez · C. R. Fadragas
Universidad Central "Marta Abreu" de Las Villas, Santa Clara, Villa Clara, Cuba
e-mail: arfivero@uclv.cu

R. Cárdenas et al. (eds.), *Proceedings of the 2nd International Conference on BioGeoSciences*, https://doi.org/10.1007/978-3-030-04233-2_2

gravity and to study the viability of that model in a Friedmann–Robertson–Walker (FRW) Universe for describing the current acceleration of the expansion of the Universe.

The Cosmological Higgs Field (CHF) is expected to exist in our Universe. This field is related to the mechanism which creates inertial mass of particles known as the Brout–Englert–Higgs mechanism [7, 8].

In the last decades, the Higgs field has been used to explain the inflationary stage of the Universe for some authors [9, 10] and it is being considered as a possibility to describe the unknown agent called "dark energy" [11], which is assumed to be the responsibility of the current accelerated expansion of the Universe.

Although we are not going to focus on this direction, it is necessary to talk about another important aspect where the CHF has a great significance. As we said before, the CHF is related to the mechanism which gives mass to subatomic particles. If particles would not have mass, the gravitational interaction between them could not be possible. Therefore, the formation of structures in the Universe would not be possible, so the Universe as we know it today would not exist, and as a result, life would not exist. Another aspect that could also change radically the face of our world is the evolution of our Universe.

In the next section, we present the construction of our model. In Sect. 3, we show the dynamical analysis of the model. In Sect. 4, we discuss the results of our analysis. Finally, we conclude in Sect. 5 with some remarks.

2 Construction of the Model with the Higgs Field in a Cosmological Background

As we suggested in the previous section, the Cosmological Higgs Field (CHF) fills the entire Universe. In the present work, we represented the CHF as described by a singlet with a $U(1)$ symmetry which is given by:

$$\Phi(t) = \frac{1}{\sqrt{2}}\phi(t)e^{i\theta(t)} \tag{1}$$

where $\phi(t)$ and $\theta(t)$ are real-valued functions of time corresponding to the amplitude and phase of the CHF, respectively. Equations of the model are derived by the traditional way considering the Lagrangian formalism. The Friedmann equations read:

$$H^2 = \frac{k}{3}\left(\frac{1}{2}\dot{\phi}^2 + \frac{1}{2}\phi^2\dot{\theta}^2 + V(\phi) + \rho\right) \tag{2}$$

$$\dot{H} = k\left(-\frac{3\gamma - 2}{6}\rho - \frac{1}{3}\dot{\phi}^2 - \frac{1}{3}\phi^2\dot{\theta}^2 + \frac{V(\phi)}{3}\right) - H^2 \tag{3}$$

The Klein–Gordon equations, for amplitude function $\phi(t)$ and for phase function $\theta(t)$, are shown as follows:

$$\ddot{\phi} + 3H\dot{\phi} - \phi\dot{\theta}^2 + \frac{\partial V}{\partial \phi} = 0 \tag{4}$$

$$\ddot{\theta} + 3H\dot{\theta} - \frac{2\dot{\phi}\dot{\theta}}{\phi} = 0 \tag{5}$$

The energy conservation equation is written as follows:

$$\dot{\rho} + 3\gamma H\rho = 0 \tag{6}$$

The self-interaction potential $V(\phi)$ [7, 11] is written as follows:

$$V(\phi) = \frac{\lambda}{4}\phi^4 - \frac{\mu^2}{2}\phi^2 + \in \tag{7}$$

Next, we elaborated the model equations in order to realize the analysis of stability from the viewpoint of the dynamical system theory. Introducing the new variables $z = \dot{\phi}$ and $w = \dot{\theta}$, and taking $k = 1$, the dynamical Eqs. (2)–(6) of the model finally take the form:

$$\dot{z} = -3Hz + \phi w^2 - \lambda\phi^3 + \mu^2\phi \tag{8}$$

$$\dot{\phi} = z \tag{9}$$

$$\dot{w} = -3Hw - \frac{2zw}{\phi} \tag{10}$$

$$\dot{\rho} = -3\gamma H\rho \tag{11}$$

$$\dot{H} = -\frac{3\gamma - 2}{6}\rho - \frac{z^2}{3} - \frac{\phi^2 w^2}{3} + \frac{\lambda}{12}\phi^4 - \frac{\mu^2}{6}\phi^2 + \frac{\in}{3} - H^2 \tag{12}$$

3 Dynamical Analysis of the Model

Now, the dynamical system technique is applied to analyze the dynamics of the CHF and its cosmological implications (see [12–15]).

Equations obtained above (8)–(12) represent a system of first-order ordinary differential equations. Time variable does not appear explicitly at the right-hand side of these equations and then one says that they represent an autonomous dynamical system. The polynomial type of the self-interacting potential considered here leads to have no advantage by introducing the usual Hubble-normalized variables.

3.1 Determination of the Critical Points

The vector field (8)–(12) of the state space has the components $[z, \phi, w, \rho, H]$. The critical points can be found if the right-hand side of each equation of the system equals zero, and they are given in Table 1.

Table 1 Critical points of the equations system and their existence

P_i	z	ϕ	w	ρ	H	Existence
P_1	0	ϕ	$-\sqrt{-\mu^2+\lambda\phi^2}$	$\frac{4\in+2\mu^2\phi^2-3\lambda\phi^4}{-4+6\gamma}$	0	$\lambda\phi^2 \geq \mu^2$ and $\gamma \neq \frac{2}{3}$
P_2	0	ϕ	$\sqrt{-\mu^2+\lambda\phi^2}$	$\frac{4\in+2\mu^2\phi^2-3\lambda\phi^4}{-4+6\gamma}$	0	$\lambda\phi^2 \geq \mu^2$ and $\gamma \neq \frac{2}{3}$
P_3	0	$-\frac{\mu}{\sqrt{\lambda}}$	0	$\frac{-4\in\lambda+\mu^4}{4\lambda-6\gamma\lambda}$	0	$\gamma \neq \frac{2}{3}$
P_4	0	$-\frac{\mu}{\sqrt{\lambda}}$	0	0	$-\frac{\sqrt{4\in\lambda-\mu^4}}{2\sqrt{3}\sqrt{\lambda}}$	$4 \in \lambda > \mu^4$
P_5	0	$-\frac{\mu}{\sqrt{\lambda}}$	0	0	$\frac{\sqrt{4\in\lambda-\mu^4}}{2\sqrt{3}\sqrt{\lambda}}$	$4 \in \lambda > \mu^4$
P_6	0	$\frac{\mu}{\sqrt{\lambda}}$	0	$\frac{-4\in\lambda+\mu^4}{4\lambda-6\gamma\lambda}$	0	$\gamma \neq \frac{2}{3}$
P_7	0	$\frac{\mu}{\sqrt{\lambda}}$	0	0	$-\frac{\sqrt{4\in\lambda-\mu^4}}{2\sqrt{3}\sqrt{\lambda}}$	$4 \in \lambda > \mu^4$
P_8	0	$\frac{\mu}{\sqrt{\lambda}}$	0	0	$\frac{\sqrt{4\in\lambda-\mu^4}}{2\sqrt{3}\sqrt{\lambda}}$	$4 \in \lambda > \mu^4$
P_9	0	$-\frac{\sqrt{\frac{\mu^2-\sqrt{\mu^4+12\in\lambda}}{\lambda}}}{\sqrt{3}}$	$-\frac{\sqrt{2\mu^2-\sqrt{\mu^4+12\in\lambda}}}{\sqrt{3}}$	0	0	Not real
P_{10}	0	$-\frac{\sqrt{\frac{\mu^2-\sqrt{\mu^4+12\in\lambda}}{\lambda}}}{\sqrt{3}}$	$\frac{\sqrt{2\mu^2-\sqrt{\mu^4+12\in\lambda}}}{\sqrt{3}}$	0	0	Not real
P_{11}	0	$\frac{\sqrt{\frac{\mu^2-\sqrt{\mu^4+12\in\lambda}}{\lambda}}}{\sqrt{3}}$	$-\frac{\sqrt{2\mu^2-\sqrt{\mu^4+12\in\lambda}}}{\sqrt{3}}$	0	0	Not real
P_{12}	0	$\frac{\sqrt{\frac{\mu^2-\sqrt{\mu^4+12\in\lambda}}{\lambda}}}{\sqrt{3}}$	$\frac{\sqrt{2\mu^2-\sqrt{\mu^4+12\in\lambda}}}{\sqrt{3}}$	0	0	Not real
P_{13}	0	$-\frac{\sqrt{\frac{\mu^2+\sqrt{\mu^4+12\in\lambda}}{\lambda}}}{\sqrt{3}}$	$-\frac{\sqrt{\sqrt{\mu^4+12\in\lambda}-2\mu^2}}{\sqrt{3}}$	0	0	$\sqrt{\mu^4+12 \in \lambda} > 2\mu^2$
P_{14}	0	$-\frac{\sqrt{\frac{\mu^2+\sqrt{\mu^4+12\in\lambda}}{\lambda}}}{\sqrt{3}}$	$\frac{\sqrt{\sqrt{\mu^4+12\in\lambda}-2\mu^2}}{\sqrt{3}}$	0	0	$\sqrt{\mu^4+12 \in \lambda} > 2\mu^2$
P_{15}	0	$\frac{\sqrt{\frac{\mu^2+\sqrt{\mu^4+12\in\lambda}}{\lambda}}}{\sqrt{3}}$	$-\frac{\sqrt{\sqrt{\mu^4+12\in\lambda}-2\mu^2}}{\sqrt{3}}$	0	0	$\sqrt{\mu^4+12 \in \lambda} > 2\mu^2$
P_{16}	0	$\frac{\sqrt{\frac{\mu^2+\sqrt{\mu^4+12\in\lambda}}{\lambda}}}{\sqrt{3}}$	$\frac{\sqrt{\sqrt{\mu^4+12\in\lambda}-2\mu^2}}{\sqrt{3}}$	0	0	$\sqrt{\mu^4+12 \in \lambda} > 2\mu^2$

3.2 Determination of the Eigenvalues for Each Critical Point

To be able to make the stability analysis of each critical point, one needs to determine the eigenvalues of the matrix of the linearization of the system (8)–(12) and evaluate the matrix at that critical point. The procedure is as follows. The system (8)–(12) must be moved to each critical point, at each time. Next, applying the perturbation technique around each critical point, we can investigate the behavior of the system around that critical point. After the origin of the differential equations is moved to the critical point considered, the linearization method is applied, and the corresponding Jacobian matrix is transformed to the Jordan canonical form. The procedure above must be applied to each critical point. In each case, the set of five eigenvalues corresponding to a given critical point is determined and then we will try to describe the behavior of the dynamics around that critical point. It will be made in the following step. In Table 2, the set of five eigenvalues for eight of the critical points is shown.

The nature of these eigenvalues determines the behavior of the dynamical system near the critical point considered. When the critical point is hyperbolic, we can apply the Hartman–Grobman theorem (see [4]).

3.3 Small Description of the Critical Points

The system (8)–(12) exhibits the set of critical points labeled P_1, P_2, …, P_{16}. The critical points P_1, P_2, P_3, P_6, P_{13}, P_{14}, P_{15}, and P_{16} have a null value for the parameter H corresponding this situation to a static Universe. The points P_4 and P_7 exhibit a negative value for the coordinate H corresponding this case to a contracting Universe. On the other hand, critical points P_5, and P_8 exhibit a positive value for the coordinate H corresponding to an expanding Universe. For all the critical points given in Table 1, the value of coordinate z always equals zero which indicates that the "translational" kinetic energy is zero.

The coordinate ϕ can take different values, and these values may be of four types (see Table 1): a negative value for the critical points P_3, P_4, and P_5, a positive value for the critical points P_6, P_7, and P_8, a different negative value for the points P_{13} and P_{14}, and a different positive value for the points P_{15} and P_{16}. Two values for coordinate ϕ correspond to points in the graphical behavior of the self-interacting potential $V(\phi)$ versus ϕ where the function exhibits extreme values. For $\phi = \pm\frac{\mu}{\sqrt{\lambda}}$, the function $V(\phi)$ has a minimum. In Table 1 are displayed the location and existence conditions of these critical points, and $V(\phi)$ and some basic observables are given in Table 3.

The critical points P_4, P_5, P_7, and P_8 exist for the condition $4 \in \lambda \geq \mu^4$. This condition corresponds to a nonnegative value of the self-interacting potential $V(\phi)$; that is, $V(\phi)$ always will be nonnegative for these critical points. The points P_3 and

Table 2 Sets of eigenvalues for the critical points of the system

$$\sum = \sqrt{-3\mu^4 - 32\lambda\mu^2 + 12 \in \lambda},$$

$$\Xi_1 = \sqrt{\lambda^2\left(216\lambda^3 \in^3 - 54\lambda^2 \in^2 \Pi_1 - 6\lambda\mu^4 \in \left(3\lambda\mu^2 - 9\lambda\sqrt{\mu^4 + 12\lambda \in} + \mu^2\sqrt{\mu^4 + 12\lambda \in}\right) + \mu^8(\mu^2 - 12\lambda)\Pi_2\right)}$$

$$\Xi_2 = \sqrt{\mu^4 + 12\lambda \in} - 9\lambda\,\Xi_3 = \mu^2 + \sqrt{\mu^4 + 12\lambda \in}, \Pi_1 = \left(-27\lambda^2 - 8\lambda\mu^2 + \mu^4 + 2\lambda\sqrt{\mu^4 + 12\lambda \in}\right)$$

$$\Pi_2 = \left(\mu^2 + \sqrt{\mu^4 + 12\lambda \in}\right)$$

P_i	λ_1	λ_2	λ_3	λ_4	λ_5
P_3	0	$-i\sqrt{2}\mu$	$i\sqrt{2}\mu$	$-\frac{\sqrt{\gamma}\sqrt{4\in\lambda-\mu^4}}{2\sqrt{\lambda}}$	$\frac{\sqrt{\gamma}\sqrt{4\in\lambda-\mu^4}}{2\sqrt{\lambda}}$
P_4	$\frac{\sqrt{4\in\lambda-\mu^4}}{\sqrt{3}\sqrt{\lambda}}$	$\frac{\sqrt{12\in\lambda-3\mu^4}}{2\sqrt{\lambda}}$	$\frac{\gamma\sqrt{12\in\lambda-3\mu^4}}{2\sqrt{\lambda}}$	$\frac{\sqrt{12\in\lambda-3\mu^4}-\sum}{4\sqrt{\lambda}}$	$\frac{\sqrt{12\in\lambda-3\mu^4}+\sum}{4\sqrt{\lambda}}$
P_5	$-\frac{\sqrt{12\in\lambda-3\mu^4}}{2\sqrt{\lambda}}$	$-\frac{\gamma\sqrt{12\in\lambda-3\mu^4}}{2\sqrt{\lambda}}$	$-\frac{\sqrt{4\in\lambda-\mu^4}}{\sqrt{3}\sqrt{\lambda}}$	$-\frac{\sqrt{12\in\lambda-3\mu^4}+\sum}{4\sqrt{\lambda}}$	$-\frac{\sqrt{12\in\lambda-3\mu^4}+\sum}{4\sqrt{\lambda}}$
P_6	0	$-i\sqrt{2}\mu$	$i\sqrt{2}\mu$	$-\frac{\sqrt{\gamma}\sqrt{4\in\lambda-\mu^4}}{2\sqrt{\lambda}}$	$\frac{\sqrt{\gamma}\sqrt{4\in\lambda-\mu^4}}{2\sqrt{\lambda}}$
P_7	$\frac{\sqrt{4\in\lambda-\mu^4}}{\sqrt{3}\sqrt{\lambda}}$	$\frac{\sqrt{12\in\lambda-3\mu^4}}{2\sqrt{\lambda}}$	$\frac{\gamma\sqrt{12\in\lambda-3\mu^4}}{2\sqrt{\lambda}}$	$\frac{\sqrt{12\in\lambda-3\mu^4}-\sum}{4\sqrt{\lambda}}$	$\frac{\sqrt{12\in\lambda-3\mu^4}+\sum}{4\sqrt{\lambda}}$
P_8	$-\frac{\sqrt{12\in\lambda-3\mu^4}}{2\sqrt{\lambda}}$	$-\frac{\gamma\sqrt{12\in\lambda-3\mu^4}}{2\sqrt{\lambda}}$	$-\frac{\sqrt{4\in\lambda-\mu^4}}{\sqrt{3}\sqrt{\lambda}}$	$-\frac{\sqrt{12\in\lambda-3\mu^4}+\sum}{4\sqrt{\lambda}}$	$-\frac{\sqrt{12\in\lambda-3\mu^4}+\sum}{4\sqrt{\lambda}}$
P_{13}	0	$\frac{-\sqrt{2}\sqrt{-\sqrt{2}\Xi_1+6\lambda^2\in\Xi_2-\lambda\mu^4\Xi_3}}{3\lambda\sqrt{\Xi_3}}$	$\frac{\sqrt{2}\sqrt{-\sqrt{2}\Xi_1+6\lambda^2\in\Xi_2-\lambda\mu^4\Xi_3}}{3\lambda\sqrt{\Xi_3}}$	$\frac{-\sqrt{2}\sqrt{\sqrt{2}\Xi_1+6\lambda^2\in\Xi_2-\lambda\mu^4\Xi_3}}{3\lambda\sqrt{\Xi_3}}$	$\frac{\sqrt{2}\sqrt{\sqrt{2}\Xi_1+6\lambda^2\in\Xi_2-\lambda\mu^4\Xi_3}}{3\lambda\sqrt{\Xi_3}}$
P_{14}	0	$\frac{-\sqrt{2}\sqrt{-\sqrt{2}\Xi_1+6\lambda^2\in\Xi_2-\lambda\mu^4\Xi_3}}{3\lambda\sqrt{\Xi_3}}$	$\frac{\sqrt{2}\sqrt{-\sqrt{2}\Xi_1+6\lambda^2\in\Xi_2-\lambda\mu^4\Xi_3}}{3\lambda\sqrt{\Xi_3}}$	$\frac{-\sqrt{2}\sqrt{\sqrt{2}\Xi_1+6\lambda^2\in\Xi_2-\lambda\mu^4\Xi_3}}{3\lambda\sqrt{\Xi_3}}$	$\frac{\sqrt{2}\sqrt{\sqrt{2}\Xi_1+6\lambda^2\in\Xi_2-\lambda\mu^4\Xi_3}}{3\lambda\sqrt{\Xi_3}}$
P_{15}	0	$\frac{-\sqrt{2}\sqrt{-\sqrt{2}\Xi_1+6\lambda^2\in\Xi_2-\lambda\mu^4\Xi_3}}{3\lambda\sqrt{\Xi_3}}$	$\frac{\sqrt{2}\sqrt{-\sqrt{2}\Xi_1+6\lambda^2\in\Xi_2-\lambda\mu^4\Xi_3}}{3\lambda\sqrt{\Xi_3}}$	$\frac{-\sqrt{2}\sqrt{\sqrt{2}\Xi_1+6\lambda^2\in\Xi_2-\lambda\mu^4\Xi_3}}{3\lambda\sqrt{\Xi_3}}$	$\frac{\sqrt{2}\sqrt{\sqrt{2}\Xi_1+6\lambda^2\in\Xi_2-\lambda\mu^4\Xi_3}}{3\lambda\sqrt{\Xi_3}}$
P_{16}	0	$\frac{-\sqrt{2}\sqrt{-\sqrt{2}\Xi_1+6\lambda^2\in\Xi_2-\lambda\mu^4\Xi_3}}{3\lambda\sqrt{\Xi_3}}$	$\frac{\sqrt{2}\sqrt{-\sqrt{2}\Xi_1+6\lambda^2\in\Xi_2-\lambda\mu^4\Xi_3}}{3\lambda\sqrt{\Xi_3}}$	$\frac{-\sqrt{2}\sqrt{\sqrt{2}\Xi_1+6\lambda^2\in\Xi_2-\lambda\mu^4\Xi_3}}{3\lambda\sqrt{\Xi_3}}$	$\frac{\sqrt{2}\sqrt{\sqrt{2}\Xi_1+6\lambda^2\in\Xi_2-\lambda\mu^4\Xi_3}}{3\lambda\sqrt{\Xi_3}}$